MODELING THE SNOW SURFACE TEMPERATURE WITH A ONE-LAYER ENERGY BALANCE SNOWMELT MODEL

Jinsheng You

School of Natural Resources, University of Nebraska – Lincoln, Lincoln, Nebraska 68583, USA (jyou2@unl.edu)

David G. Tarboton

Civil and Environmental Engineering, Utah State University, Logan, Utah 84322, USA (dtarb@usu.edu), telephone: 435-797-3172, Fax: 435-797-1185

Charles H. Luce

USDA Forest Service, Rocky Mountain Research Station, 322 E Front St., Boise, ID 83702 USA (cluce@fs.fed.us)

Short title: Utah Energy Balance snowmelt model

Abstract

Snow surface temperature is a key control on and result of dynamically coupled energy exchanges at the snow surface. The snow surface temperature is the result of the balance between external forcing (incoming radiation) and energy exchanges above the surface that depend on surface temperature (outgoing longwave radiation and turbulent fluxes) and the transport of energy into the snow by conduction and meltwater influx. Because of the strong insulating properties of snow, thermal gradients in snow packs are large and nonlinear, a fact that has led many to advocate multiple layer snowmelt models over single layer models. In an effort to keep snowmelt modeling simple and parsimonious, the Utah Energy Balance (UEB) snowmelt model used only one layer but allowed the snow surface temperature to be different from the snow average temperature by using an equilibrium gradient parameterization based on the surface energy balance. Although this procedure was considered an improvement over the ordinary single layer snowmelt models, it still resulted in discrepancies between modeled and measured snowpack energy contents. In this paper we evaluate the equilibrium gradient approach, the force-restore approach, and a modified force-restore approach when they are integrated as part of a complete energy and mass balance snowmelt model. The force-restore and modified force-restore approaches have not been incorporated into the UEB in early versions, even though Luce and Tartoton have done work in calculating the energy components using these approaches.. In addition, we evaluate a scheme for representing the penetration of a refreezing front in cold periods following melt. We introduce a method to adjust effective conductivity to account for the presence of ground near to a shallow snow surface. These parameterizations were tested against data from the Central Sierra Snow Laboratory, CA, Utah State University experimental farm, UT, and Subnivean snow laboratory at Niwot Ridge, CO. These tests compare modeled and measured snow surface temperature, snow energy content, snow water equivalent, and snowmelt outflow. We found that with these refinements the model is able to better represent the snowpack energy balance and internal energy content while still retaining a parsimonious one layer format.

Keyword: Energy Balance snowmelt model, refreezing, snow, snow water equivalent, surface temperature of snow.

1. Introduction

Snowmelt is an important source of water in the western United States and much of the world. Modeling snowmelt is important for water resources management and the assessment of spring snowmelt flood risk. The processes involved in snowmelt have been widely described (U.S. Army Corps of Engineers, 1956; Gray and Male, 1981; Bras, 1990; Dingman, 1994; Linsley *et al.*, 1975; Viessman *et al.*, 2002). In snowmelt modeling, the heat flux between the snowpack and the atmosphere is partially governed by the snow surface temperature (Gray and Male, 1981; Dingman, 1994; Dozier, 1989) which depends on the conductive heat flux into the snow. Modeling conductive heat flux through the snowpack is a complex problem due to the changing nature of the snowpack through the influences of heating and cooling history. One of the primary reasons for the poor performance of single layer models in comparative validations is the poor representation of internal snowpack heat transfer processes (Blöschl and Kirnbauer, 1991; Koivasulo and Heikenkeimo, 1999). Some snowmelt models use finite difference solutions of the heat equation (Anderson, 1976; Dickinson *et al.*, 1993; Flerchinger and Saxton, 1989; Jordan, 1991; Yen, 1967). Possible inaccuracies in modeling the internal snowpack properties could lead to errors in estimating the snowpack and snow surface temperature (Colbeck and Anderson, 1982). Models such as CROCUS (Vionnet *et al*., 2012) have made considerable progress in representing the detail of within snow processes. There has also been recent progress towards using Richards equation to model meltwater flow in snow using multiple layers (Wever *et al*., 2014). However Wever *et al*., did note that there are challenging numerical issues associated with inhomogeneities in grain size and density, and precise quantification of the parameters that impact the model is a challenge. Furthermore, there is an increasing realization that lateral inhomogeneities in snowpacks are important (e.g. Wankiewicz, 1979; Higuchi and Tanaka, 1982; Kattelmann and Dozier, 1999; Williams et al., 2010; and Eiriksson et al., 2013). These inhomogeneities result in lateral variability across a range of scales and fingering in the way that meltwater enters and flows through snow that is different from the matrix flow represented in one-dimensional finite difference solutions. This suggests that even our most complex snowpack models must seek a way to parameterize unmeasurable sub-element scale variability due to the difficulties in intensive field work. In the single layer approach we model the surface temperature that provides the connection between the snow and the atmosphere above with a relatively straightforward way to avoid modeling the complexity of processes.

Modeling needs a balance between representing details that are important to the purpose, or question being addressed and avoiding complexity and inaccuracy for details that are less important. There is no one right solution and in this paper we examine and evaluate single layer solutions that avoid some of the complexity of multilayer models for our purposes, which are the quantification of overall surface energy exchanges and meltwater produced by a snowmelt model for hydrological studies.

The UEB snowmelt model (Tarboton *et al.*, 1995; Tarboton and Luce, 1996, You 2004) is a physically-based point energy and mass balance model for snow accumulation and melt. The snowpack is characterized using two primary state variables, namely, snow water equivalent, W, (m) and the internal energy of the snowpack and top layer of soil, U, (kJ m^{-2}). The physical basis of the model is the conservation of mass and energy. Snow surface temperature, a key variable in calculating latent and sensible heat fluxes and outgoing longwave radiation, is modeled using a thin surface skin or equilibrium gradient approach. The surface skin is assumed to have zero heat capacity. Snow surface temperature is calculated from the energy balance at the surface of the snowpack by equating incoming and outgoing fluxes between the snow mass and the air above; this allows the snow surface skin temperature to be different from the average temperature of the snowpack as reflected by the energy content. This thus reflects the key insulating effect of snow on the surface energy balance without the introduction of additional layers and their resultant complexity and the potential for error where there is insufficient information to properly model this complexity.

The UEB model was initially tested against snow accumulation and melt measurements and was found to perform well. Later tests included comparisons against internal energy through measurement of the temperature profile in a snowpack (Tarboton, 1994). These tests indicated a discrepancy between the modeled and the measured internal energy (Tarboton, 1994; Tarboton and Luce, 1996). Luce (2000) and Luce and Tarboton (2010) analyzed the snowpack energy fluxes from a season of measurements collected at the USU drainage farm in Cache Valley, Utah to evaluate the reasons for the discrepancies in the internal energy. One cause was the estimation of longwave radiation inputs based on air temperatures in an environment subject to frequent temperature inversions and resultant fog. Another cause of the discrepancies was the parameterization of snow surface temperature. These problems had been offsetting each other in a way that when the longwave radiation inputs were corrected, the modeled surface temperatures no longer matched measurements. To address this problem, Luce (2000) and Luce and Tarboton (2001, 2010) evaluated various alternative parameterizations against the currently used equilibrium gradient approach. These included the force-restore approach (e.g. Deardorff, 1978; Dickinson *et al.*, 1993; Hu and Islam, 1995) and a modified force-restore approach that was suggested (Luce 2000; Luce and Tarboton, 2001, 2010) to improve the representation of snow surface temperature and help improve the representation of energy content in the snowpack. However these evaluations were driven by measured surface temperature and did not include coupled modeling of the snow energy balance driven by atmospheric forcing. In this paper these suggestions are implemented and tested within the UEB snowmelt model.

Snowmelt generated at the snow surface is initially held in the snowpack as liquid water up to the liquid holding capacity. When the surface forcing changes to cooling, this water refreezes and a refreezing front penetrates into the snow. The rate of penetration of the refreezing front is governed by the rate of heat loss, the latent heat of fusion, and the temperature gradient in the layer above the refreezing front. The original UEB model (Tarboton, 1994; Tarboton and Luce, 1996) used the equilibrium gradient approach to estimate snow surface temperature and did not account for the presence of liquid water during refreezing periods with the result that the snow surface temperature is modeled as too low with too little heat loss during these periods. Multiple-layer snow models (e.g. Flerchinger and Saxton, 1989; Jordan, 1991) account for this effect because the liquid content and temperature of each layer is explicitly represented. Here we present and test a formulation for representing this refreezing effect in the single layer UEB model. In addition to the two changes mentioned above we also introduce a method to adjust the effective thermal conductivity of shallow snowpacks to account for the combined effect of snow and the ground below the snow.

2. Model Description

2.1 Mass and energy balance equations

The original UEB model is described by Tarboton *et al.*, (1995) and Tarboton and Luce (1996). Here we evaluate modifications introduced to refine the representation of surface temperature, including the modified force-restore approach, refreezing of liquid water and conductivity adjustments for shallow snow (You, 2004). In separate work, we have evaluated the addition of a vegetation layer to UEB (Mahat and Tarboton, 2012; Mahat et al., 2013). We refer to the Tarboton *et al.*, (1995) model as the *original* UEB model. The model examined here we refer to as *surface* UEB. This is a single layer model used to model snow accumulation in the open and is also the beneath canopy part of *vegetation* UEB that models snow accumulation and melt in forested environments. Vegetation UEB comprises two layers, a surface layer that is surface UEB and a vegetation layer that was evaluated by Mahat and Tarboton (2012) and Mahat et al., (2013). A comprehensive review of the surface layer model is given here so that the reader can understand the context for the modifications that were made. Where we do not use a qualifier the methods are the same in surface UEB and the original UEB.

In the UEB model (Tarboton *et al.*, 1995; Tarboton and Luce, 1996), the time evolution of the snowpack is driven by the energy exchange between the snowpack, the air above and the soil below according to mass and energy balance equations through snow water equivalent, W, and energy content, U,

$$\frac{dU}{dt} = Q_{sn} + Q_{li} - Q_{le} + Q_p + Q_g + Q_h + Q_e - Q_m, \quad (\text{kJ m}^{-2}\ \text{h}^{-1}) \qquad (1)$$

$$\frac{dW}{dt} = P_r + P_s - M_r - E, \quad (\text{m h}^{-1}) \qquad (2)$$

where Q_{sn} is the net shortwave energy received by the snowpack, Q_{li} is the incoming longwave radiation, Q_{le} is outgoing longwave radiation, Q_p is the energy advected by precipitation into the snow, Q_g is the ground heat flux to the combination of snow and the upper layer of soil, Q_h is the sensible heat flux to/from the snow with sign convention that flux to the snow is positive, Q_e is the latent heat flux to/from the snow with sign convention that flux to the snow is positive, and Q_m is the advected heat removed by meltwater. P_r is the rate of precipitation as rain; P_s is the rate of precipitation as snow; M_r is the meltwater outflow rate; and E is the sublimation rate; t is time (h). Internal energy U is not defined relative to absolute zero, but rather relative to the melting point. U is thus taken as 0 kJ m^{-2} when the snowpack is frozen at 0 ^{o}C and contains no liquid water. With this definition negative internal energies correspond to the cold content (e.g., Dingman, 1994 p182) and positive internal energies reflect change in phase of some fraction of snow from frozen to liquid. The model requires inputs of air temperature, wind speed, humidity, and incident radiation that are used to drive the energy balance, and precipitation that is used to drive the mass balance. Precipitation is partitioned into snowfall or rainfall based upon air temperature (U.S. Army Corps of Engineers, 1956). In locations where snow is subject to redistribution due to wind blown drifting or sliding, an accumulation factor (Tarboton *et al.*, 1995; Tarboton and Luce, 1996; Luce et al., 1998) is used to adjust the snowfall inputs.

The use of energy content as a state variable means that the model does not explicitly prognose snowpack temperature. Since snowpack temperature is important for energy fluxes into the snow, it needs to be obtained diagnostically from internal energy and snow water equivalent as follows:

If $U < 0$ $$T_{ave} = U / \left(\rho_w W C_i + \rho_g D_e C_g\right)$$ All solid phase (3 a)

If $0<U<\rho_w W h_f$ $$T_{ave} = 0°C \text{ with } L_f = U/(\rho_w h_f W)$$ Solid and liquid mixture (3 b)

If $U>\rho_w W h_f$ $$T_{ave} = \frac{U - \rho_w W h_f}{\rho_g D_e C_g + \rho_w W C_w}$$ All liquid (3 c)

In the equations above, T_{ave} denotes snowpack average temperature (^{o}C), h_f denotes the latent heat of fusion (333.5 kJ kg^{-1}), ρ_w the density of water (1000 kg m^{-3}), C_i the specific heat of ice (2.09 kJ kg^{-1} °C^{-1}), ρ_g the soil density, C_g the specific heat of soil, C_w the specific heat of water (4.18 kJ kg^{-1} °C^{-1}), D_e the depth of soil that interacts thermally with the snowpack and L_f the liquid fraction by mass. The basis for equations (3 a) to (3 c) is that the heat required to melt the entire snow water equivalent at 0 °C is $\rho_w W h_f$ (kJ m^{-2}). Where U is between 0 and this quantity, the liquid fraction is determined by proportioning, i.e. $L_f = U/(\rho_w h_f W)$. The heat capacity of the snow combined with thermally interacting soil layer is $\rho_w W C_i + \rho_g D_e C_g$ (kJ °C^{-1}m^{-2}), so in the case that $U<0$, dividing U by this combined heat capacity gives T_{ave}. Where $U> \rho_w W h_f$ the snow contains sufficient energy to melt completely and the temperature of the remaining liquid phase is given by (3 c). Practically, the condition in Equation (3 c) only occurs when W is zero since a completely liquid snowpack cannot exist; it becomes melt runoff. Nevertheless, this equation is included for completeness to keep track of the energy content during periods of intermittent snow cover. With T_{ave} representing the temperature of the ground, Eq. (3c) handles the possibility of snowfall melting immediately due to coming in contact with warm ground.

The net shortwave radiation is calculated from incident shortwave radiation and albedo calculated as a function of snow age and solar illumination angle following Dickinson *et al*. (1993). The incident shortwave radiation is either measured or estimated from the diurnal temperature range (Bristow and Campbell, 1984). On sloping surfaces, incident radiation is adjusted for slope and aspect (e.g. Dingman, 1994).

In the albedo model, which follows Dickinson *et al*. (1993) and is described in detail in Tarboton and Luce (1996), the dimensionless age of the snow surface, τ, is retained as a state variable, and is updated with each time step, dependent on snow surface temperature and snowfall. Reflectance is computed for two bands; visible (< 0.7 µm) and near infrared (> 0.7 µm) with adjustments for illumination angle and snow age. Then albedo is taken as the average of the two reflectances. A parameter d_{NewS} (m) represents the depth of snowfall that is assumed to restore the snow surface to new conditions ($\tau = 0$). With snowfall, P_s, less than d_{NewS} in a time step the dimensionless age is reduced by a factor $(1-P_s/d_{NewS})$

When the snowpack is shallow (depth $z < h = 0.1$ m) the effective surface albedo, A, is taken as $r_\alpha \alpha_{bg}+(1-r_\alpha)\alpha_s$ where $r_\alpha=(1-z/h)e^{-z/2h}$. This interpolates between the snow albedo, α_s, and bare ground albedo, α_{bg}, with the exponential term approximating the exponential extinction of radiation penetration of snow scaled to $1/e^2$ at depth h.

The incident longwave radiation is estimated based on air temperature, T_a (K) using the Stefan-Boltzmann equation. The emissivity of air is estimated using Satterlund's (1979) equation for clear conditions. The presence of clouds increases downward longwave radiation. This is modeled by estimating the cloud cover fraction based on the Bristow and Campbell (1984) atmospheric transmission factor (see details in Tarboton and Luce, 1996) . The outgoing longwave radiation is calculated from the snow surface temperature using the Stefan-Boltzmann equation, with emissivity of snow, ε_s, taken as 0.99.

The latent heat flux, Q_e and sensible heat flux, Q_h are modeled using bulk aerodynamic formulae (Anderson, 1976):

$$Q_h = \rho_a C_p (T_a - T_s) K_h \quad (4)$$

and

$$Q_e = \rho_a h_v (q_s - q_a) K_e, \quad (5)$$

where ρ_a is the density of air, C_p is the specific heat of air at constant pressure (1.005 kJ kg^{-1} $^{o}C^{-1}$), h_v is the latent heat of vaporization (sublimation) of ice (2834 kJ kg^{-1}), q_a is the air specific humidity, q_s is the specific humidity at the snow surface which is assumed to be saturated relative to the vapor pressure over ice (e.g., Lowe, 1977), and K_h and K_e are turbulent transfer conductances for sensible and latent heat respectively. Under neutral atmospheric conditions K_e and K_h are given by

$$K_n = \frac{k_v^2 u}{[\ln(z_m / z_0)]^2} \quad (6)$$

where z_m is the measurement height for wind speed, air temperature, and humidity, u is the wind speed, k_v is von Kármán’s constant (0.4), and z_0 is the aerodynamic roughness. When there is a temperature gradient near the surface, buoyancy effects may enhance or dampen the turbulent transfers, necessitating adjustments to K_n. We use

$$K_h = K_n \frac{1}{\Phi_M \Phi_H} \quad (7)$$

and

$$K_e = K_n \frac{1}{\Phi_M \Phi_E} \tag{8}$$

where Φ_M, Φ_H, Φ_E are the stability functions for momentum, sensible heat, and water vapor, respectively. The stability functions are estimated using the bulk Richardson number:

$$R_i = \frac{g z_m (T_a - T_s)}{\frac{1}{2}(T_a + T_s) u^2}, \tag{9}$$

where g is gravity acceleration (9.8 m s^{-2}). For stable conditions (R_i>0), we use the approximation of Price and Dunne (1976),

$$\frac{1}{\Phi_M \Phi_H} = \frac{1}{\Phi_M \Phi_E} = \frac{1}{1+10R_i}. \tag{10}$$

For unstable conditions (R_i<0) we use (Dyer and Hicks, 1970; Anderson, 1976; Jordan, 1991),

$$\frac{1}{\Phi_M \Phi_H} = \frac{1}{\Phi_M \Phi_E} = (1-16R_i)^{0.75}. \tag{11}$$

Because information for estimating turbulence under extremely unstable conditions is poor, we capped the value of $1/\Phi_M\Phi_H$ at 3, which occurs near R_i = -0.2. Anderson (1976) shows that iterative solutions of Deardorff's (1968) empirical equations begin to level off for more strongly unstable situations as the value of 3 is approached. Strongly unstable conditions are rare over snow, but this is in the model code for completeness. These stability corrections assume that sensible and latent heat transfer coefficients are equal, K_h=K_e.

2.2 Original quantification of surface energy flux

An important characteristic of the UEB model is its separate representation of surface temperature and average snowpack temperature. This facilitates reasonable modeling of surface energy exchanges that depend on snow surface temperature, while retaining a parsimonious single layer model. In this paper we apply new parameterizations for the snow surface temperature introduced by Luce and Tarboton (2010) and test them in the context of a full surface energy balance. The sum of energy fluxes in Equation (1) from above the snowpack are referred to as the surface energy forcing.

$$Q_{forcing}(T_s) = Q_{sn} + Q_{li} + Q_h(T_s) + Q_e(T_s) + Q_p - Q_{le}(T_s) \qquad (12)$$

The sensible heat, latent heat, and outgoing longwave radiation are functionally dependent on the surface temperature, T_s. In the original model, the heat conducted into the snow, Q_{cs}, is calculated as a function of the snow surface temperature, T_s, and average snowpack temperature, T_{ave}.

$$Q_{cs}(T_s, T_{ave}) = k\rho_s C_i \frac{(T_s - T_{ave})}{Z_e} = K_s \rho_s C_i (T_s - T_{ave}) \quad (13)$$

where ρ_s is the snow density (kg m^{-3}), k the snow thermal diffusivity (m^2 h^{-1}), Z_e the effective depth over which the temperature gradient acts (m), and $K_s=k/Z_e$ is termed snow surface conductance. In the original model, because there is uncertainty in values for Z_e and k, K_s was used as a calibration parameter.

The energy balance at the surface is given by:

$$Q_{cs}(T_s, T_{ave}) = Q_{forcing}(T_s). \quad (14)$$

Equation (14) is solved numerically for T_s using the Newton-Raphson method backed up by a more robust bisection approach. The Newton-Rhapson scheme is used first because it is more efficient. It tests for convergence and in time steps (a small percentage depending on the data) when it does not converge, the model resorts to a more robust bisection approach that is guaranteed to converge because the equation giving temperature flux into the snow based on surface temperature is monotonic. This is the case for all the surface temperature parameterizations evaluated. Thus the new approach for surface temperature does not alter the numerical stability. Physically, T_s is constrained to be no greater than 0 ^{o}C when there is snow present. When the equilibrium solution produces a solution of T_s>0^{o}C, this means that conduction into the snow cannot accommodate all the energy input through surface forcing, and the extra energy will produce meltwater at the surface, which then infiltrates into the lower parts of the snowpack and, if U<0, refreezes, representing the meltwater advection process for transport of energy into the snow. In these cases the surface energy flux terms in Equation (1) are calculated using $T_s = 0\ ^oC$ to model the snow energy content change.

3. Alternative Models of Surface Heat Conduction

Heat flow in a snowpack can be described using the diffusive heat transfer equation and assuming homogeneity of snow properties (Yen, 1967)

$$\frac{\partial T}{\partial t} = k \frac{\partial^2 T}{\partial z^2}, \qquad (15)$$

where T is the temperature (^{o}C), z is depth relative to snow surface (m), and k is the thermal diffusivity of snow (m^2 h^{-1}). Thermal diffusivity is related to thermal conductivity and specific heat by:

$$k = \frac{\lambda}{C_i \rho_s}, \qquad (16)$$

where λ is the thermal conductivity of snow (kJ m^{-1} K^{-1} h^{-1}). For semi-infinite boundary conditions ($0<z<\infty$) with sinusoidal temperature fluctuation at the upper boundary (z=0):

$$T(0,t) = \langle T \rangle + A\sin(\omega t), \tag{17}$$

the differential equation (15) has solution (Berg and McGregor, 1966):

$$T(z,t) = \langle T \rangle + Ae^{-\frac{z}{d}} \sin\left(\omega_1 t - \frac{z}{d}\right) \tag{18}$$

In this solution, A is the amplitude of the imposed temperature fluctuation at the surface, ω is the frequency, $\langle T \rangle$, the average about which surface temperature fluctuations are centered, and d is the damping depth for a given frequency. At the snow surface, the primary forcing is diurnal, suggesting $\omega=\omega_1=2\pi/24\ h^{-1}$, with the damping depth, $d = d_1 = \sqrt{\frac{2k}{\omega_1}}$, corresponding to frequency ω_1.

Equation (18) indicates that temperature oscillations are damped by a factor $1/e$ for each increment of depth d_1, and the time-averaged temperature at each depth is $\langle T \rangle$. Equation (18) can be differentiated on the depth (z) to evaluate the temperature gradient, and the surface energy flux (at z=0) can be written as:

$$Q_{cs} = -\lambda \frac{\partial T}{\partial z}(0,t) = \frac{\lambda A}{d_1}\left[\sin(\omega_1 t) + \cos(\omega_1 t)\right]. \tag{19}$$

Recognizing that $\omega_1 cos(\omega_1 t)$ is the derivative of $sin(\omega_1 t)$ with respect to t, and substituting Equation (17) and its time derivative into Equation (19) yields:

$$Q_{cs} = \frac{\lambda}{d_1 \omega_1} \frac{\partial T}{\partial t}(0,t) + \frac{\lambda}{d_1}\left(T(0,t) - \langle T \rangle\right). \tag{20}$$

This expresses the surface heat flux as a function of both the time derivative of surface temperature and the difference between the current surface temperature and the time averaged surface temperature (Luce and Tarboton, 2010). This analytic solution for the simplified setting of a semi-infinite domain with sinusoidal surface temperature forcing serves as the basis for the numerical approximations of surface temperature, T_s, that are evaluated.

3.1 Equilibrium gradient approach

The original equilibrium gradient method of surface temperature parameterization used in Equation (13) can be seen to be an approximation to Equation (20) that ignores the time derivative of the surface temperature term and approximates the average temperature at the surface over time, $\langle T \rangle$, by the snowpack average temperature, T_{ave}, while using actual surface temperature, T_s, in place of the sinusoidal forcing $T(0,t)$. This method approximates the energy flux as a gradient between the surface temperature and average temperature of snow over an effective distance Z_e, equivalent to d_1. In the original UEB model Z_e was absorbed into the parameter K_s that was calibrated, however here d_1 is related to the diurnal frequency, so to retain this calibration capability we use $Z_e = rd_1$ (i.e., the damping depth d_1 scaled by a dimensionless adjustable parameter r) and write Equation (13) in the form showing the similarity to Equation (20):

$$Q_{cs} = \frac{\lambda}{rd_1}\left(T_s - T_{ave}\right). \tag{21}$$

3.2 Force-restore approach

The force-restore parameterization (e.g. Deardorff, 1978; Dickinson *et al.*, 1993; Hu and Islam, 1995) is:

$$Q_{cs} = \frac{\lambda}{d_1}\frac{1}{\omega_1 \Delta t}\left(T_s - T_{s_{lag1}}\right) + \frac{\lambda}{rd_1}\left(T_s - T_{ave}\right), \tag{22}$$

(Luce and Tarbton, 2010). Here Δt is the time step and T_{slag1} is the surface temperature of snow in the previous time step. A finite difference approximation has been used for the time derivative and $\langle T \rangle$ has been replaced by the depth average snowpack temperature T_{ave}. Again, we have scaled the damping depth by a parameter r.

3.3 Modified force-restore approach

Luce (2000) and Luce and Tarboton (2001; 2010) found that the diurnal cycle may be superimposed on a temperature gradient that varied at longer weekly to seasonal time scales, causing variations in the temperature gradient and heat fluxes with depth. Luce (2000) and Luce and Tarboton (2001; 2010) suggested that the heat flux and the surface temperature could be estimated using the following modification to the force-restore equation:

$$Q_{cs} = \frac{\lambda}{d_1}\frac{1}{\omega_1 \Delta t}\left(T_s - T_{s_{lag1}}\right) + \frac{\lambda}{rd_1}\left(T_s - \overline{T}_s\right) + \frac{\lambda}{d_{lf}}\left(\overline{T}_s - \overline{T}_{ave}\right), \qquad (23)$$

where $\overline{T}_s$ is the average surface temperature estimated for the previous 24 hours, and $\overline{T}_{ave}$ is the 24 hour time average of the depth average snowpack temperature. The 3rd term represents the superimposed gradient, a lower frequency effect, approximated using an equilibrium gradient approach similar to Equation (21). In this parameterization d_{lf} is the damping depth associated with the longer time scale forcing having lower frequency ω_{lf}, i.e. $d_{lf} = \sqrt{\frac{2k}{\omega_{lf}}}$. In Equation (23) since the appropriate low frequency parameter (ω_{lf}) is not known *a priori*, Luce (2000) and Luce and Tarboton (2001; 2010) suggested that d_{lf} be calibrated.

3.4 Theory of meltwater refreezing

The approaches described above solve for surface temperature based upon a balance between surface forcing and the capacity of the snow near the surface to conduct heat into or out of the snowpack. However, during a cooling period following melting where there is liquid water present in the snow, the depression of snow surface temperature is inhibited by the energy required to refreeze liquid water near the surface before a temperature gradient can be established and conduction can occur. The net effect of this is that when there is liquid water present the snow surface stays warmer longer and heat loss at night and in cooling periods is more rapid. To accommodate this effect we have developed a parameterization for the penetration of a refreezing front and conduction of heat between the surface and refreezing front while there is liquid water present in the snow.

When snow energy content U is greater than 0, liquid water exists in the snowpack. The snowpack is assumed to be isothermal at 0 ^{o}C. Using the relationship between energy content and liquid fraction (Equation 3 b), the equivalent depth of liquid water in the snowpack w_m (m) is calculated as:

$$w_m = L_f W = \frac{U}{\rho_w h_f} \tag{24}$$

The capillary holding capacity of the snow is defined as mass fraction liquid holding capacity, L_c, times snow water equivalent L_cW, which implies that the maximum density of capillary water, ρ_m, is $\rho_m = \frac{L_c W \rho_w}{D} = L_c \rho_s$, where D is the depth of snowpack. We assume that prior to melt outflow, when the liquid water content is less than the capillary holding capacity, the meltwater is held at the maximum density of capillary water in the upper portion of the snowpack. The justification for this assumption is that energy generating melt primarily originates at the surface. With this assumption the depth to which meltwater has penetrated is:

$$d_w = \frac{w_m \rho_w}{\rho_m} = \frac{U}{\rho_w h_f} \frac{\rho_w}{\rho_m} = \frac{U}{\rho_m h_f}. \qquad (25)$$

This describes the state of the snowpack prior to the onset of a refreezing episode during which $Q_{forcing}$ is negative. The negative forcing will result in refreezing that penetrates down from the surface as illustrated in Figure 1. The rate of increase of the depth to the refreezing front, d_r, is given by:

$$\frac{dd_r}{dt} = -\frac{Q(T_S)}{\rho_m h_f}, \qquad (26)$$

where $Q(T_s)$ is the heat flux just above the refreezing front, here indicated to be a function of surface temperature T_s. The sign convention is that heat flux is positive into the snow which is why there is a negative sign in Equation (26).

We assume a linear temperature gradient above the refreezing front with $Q(T_s)$ given by

$$Q(T_s) = \lambda \frac{T_s}{d_r}. \qquad (27)$$

We use an equilibrium approach for surface temperature that balances the surface forcing with the conduction into the snow above the refreezing front, neglecting any heat stored in the snow between the refreezing front and the surface (as this will be small because the heat capacity of snow is less than the latent heat of fusion). This is written

$$Q(T_s) = Q_{forcing}(T_s)\,. \tag{28}$$

To solve for $d_r(t)$ the dependence of $Q_{forcing}(T_s)$ on T_s is linearized,

$$Q_{forcing}(T_s) = a - bT_s\,. \tag{29}$$

Here a is the forcing surface energy flux when the surface temperature of snow is 0 ^{o}C, and b is the slope of surface forcing flux to surface temperature function. This is a positive value since $Q(T_s)$ decreases with T_s. a is obtained by putting T_s=0 into $Q_{forcing}(T_s)$. b is obtained by putting a small negative (below freezing) T_s into $Q_{forcing}(T_s)$ and solving (29). If a is greater than 0, then the surface forcing is positive and meltwater is being generated at the surface so d_r is set to 0. When a becomes less than 0, the snowpack starts refreezing. Combining Equations (27) and (29) gives:

$$\frac{\lambda}{d_r} T_s = a - bT_s\,, \tag{30}$$

T_s can then be expressed as:

$$T_s = \frac{a}{\frac{\lambda}{d_r} + b} . \qquad (31)$$

Substituting this T_s into (27) then the result into (26) gives:

$$\frac{dd_r}{dt} = -\frac{\lambda a}{\rho_m h_f (\lambda + b d_r)} , \qquad (32)$$

Integrating Equation (32) starting from the initial refreezing depth d_{r1} during a time step, we get:

$$\lambda d_r + \frac{b}{2} d_r^{\ 2} - (\lambda d_{r1} + \frac{b}{2} d_{r1}^{\ 2}) = -\frac{a\lambda}{\rho_m h_f} \Delta t \qquad (33)$$

This has solution

$$d_r = \frac{-\lambda + \sqrt{\lambda^2 + 2b(\lambda d_{r1} + \frac{b}{2} d_{r1}^{\ 2} - \frac{a\lambda\Delta t}{\rho_m h_f})}}{b} . \qquad (34)$$

Only the positive root has been retained since only positive values of d_r are physically interpretable and b is a value greater than 0. When d_r is greater than rd_1, the effective depth associated with diurnal temperature fluctuations, or all meltwater is refrozen, the model reverts back to the surface temperature parameterization without refreezing of meltwater as described above.

3.5 Adjustment of thermal conductivity, λ, for shallow snowpack

In equations (13), (21), (22) and (23) the temperature gradient is calculated over an effective depth ($Z_e = rd_1$) estimated from the depth of penetration of surface temperature forcing at a diurnal frequency. When the snow is shallow this depth may extend into the ground below the snow cover. In such cases the thermal conductivity used in the surface temperature parameterizations above needs to reflect the combined conductivity of snow and soil below. We therefore take the effective thermal conductivity of the snowpack, λ_e, as the harmonic mean to the effective depth, Z_e, where the amplitude is damped by the same factor as it would be for deep snow (see Figure 2). In deep snow the amplitude of diurnal temperature fluctuations at depth Z_e is damped by (Equation 18) $e^{-Z_e/d_1} = e^{-r}$. In the combined snow/soil system, given r, we first solve for the depth into the soil z_2 at which the amplitude of diurnal temperature fluctuations is damped by this same factor e^{-r}. Then λ_e is obtained by taking the harmonic mean to this depth. The thermal diffusivity of the ground below the snow, k_g, is related to the thermal conductivity, λ_g, heat capacity, C_g, and density, ρ_g, of the ground through:

$$k_g = \frac{\lambda_g}{C_g \rho_g}. \qquad (35)$$

The diurnal damping depth, d_g, associated with this ground thermal diffusivity is:

$$d_g = \sqrt{\frac{2k_g}{\omega_1}} . \qquad (36)$$

The amplitude of diurnal temperature fluctuation at depth z_2 into the ground, relative to the surface temperature fluctuation is therefore damped by $e^{-z_s/d_1} e^{-z_2/d_g}$. Equating this to e^{-r} we obtain:

$$\frac{z_s}{d_1} + \frac{z_2}{d_g} = r . \qquad (37)$$

Thus z_2 is:

$$z_2 = d_g (r - \frac{z_s}{d_1}) . \qquad (38)$$

The effective thermal conductivity, λ_e, and the effective depth, Z_e, for the shallow snowpack are then estimated through:

$$Z_e = z_s + z_2 = z_s + d_g (r - \frac{z_s}{d_1}) , \qquad (39)$$

$$\frac{1}{\lambda_e} = \frac{\frac{z_s}{\lambda} + \frac{z_2}{\lambda_g}}{Z_e}, \tag{40}$$

Equation (40) is used to obtain the effective thermal conductivity near the surface when the snow is shallow. This is used in the parameterizations for surface temperature that calculate the surface heat flux between the snowpack and the atmosphere as well as conduction into the snow.

Summarizing our model improvements, the force restore and modified force restore approach have been included in the new surface UEB snowmelt model to better parameterize the surface temperature of snow. A new refreezing scheme was developed to model heat loss following partial melt through modeling the penetration of a refreezing front into the snowpack. The model was changed to adjust effective thermal conductivity used in the surface temperature parameterization for a shallow snowpack where the penetration depth for diurnal temperature fluctuations extends into the ground.

4. Study Sites and Data

The new surface UEB model was calibrated and tested using data from three locations in the Western U.S.

Utah State University Drainage and Evapotranspiration Experimental Farm.

The USU drainage and evapotranspiration experimental farm is located in Cache Valley near Logan, Utah, USA (41.6° N, 111.6° W, 1350 m elevation). The weather station and instrumentation were in a small fenced enclosure at the center of an open field with no obstructions to wind in any direction for at least 500 m. Cache Valley is a flat-bottomed valley surrounded by mountains that reach elevations of 3000 m. During the period of this experiment the ground was snow covered from November 20, 1992 to March 22, 1993. Air temperatures ranged from -23 °C to 16 °C and there was 190 mm of precipitation (mostly snow, but some rain). The snow accumulated to a maximum depth of 0.5 m with maximum water equivalent of 0.14 m. Data collected included measurements of snow water equivalent, snow surface temperature, temperatures within the snowpack and the upper soil layer, and the meteorological variables necessary to drive UEB at 30 minute time steps.

Shallow soil temperatures were measured using two thermocouples placed below the ground surface at depths of 25 mm and 75 mm. Another thermocouple was placed at the ground surface. The snowpack temperature was measured using thermocouples suspended at 50, 125, 200, 275 and 350 mm above the ground surface on fishing line strung between two upright posts. These temperature measurements were corrected for high frequency fluctuations in the panel reference temperature (Luce and Tarboton 2010). Snowpack surface temperature was measured with two Everest Interscience model 4000 infrared thermometers. Internal energy content of the snowpack was calculated from the temperature profile of the snowpack and upper soil layer accounting for the near surface nonlinearity through an analytic integral of Equation (18) as described by Luce (2000), Luce and Tarboton (2010). Snow water equivalent was measured using a snow tube. Snow pits provided measurements of density and depth. On each measurement occasion snow water equivalent was measured at eight locations (fewer when snow had disappeared from some) and averaged.

A complete dataset including the air temperature, wind speed, relative humidity, incident shortwave radiation, outgoing shortwave radiation, temperature profile through the snow and surface temperature of snowpack was available from January 26, 1993 to March 22, 1993 when the snow completely melted away. The data at USU DF was used in this study to calibrate the new surface UEB model.

Central Sierra Snow Laboratory

The Central Sierra Snow Laboratory located 1 km east of Soda Springs, California, measures and archives comprehensive data relevant to snow. It is located at 39˚19′ N, 120°22′ W, at an elevation of 2100 m. The meteorological data are reported each hour and consist of temperature, radiation, humidity, precipitation, and wind measurements at two levels in a 40 m by 50 m clearing and in a mixed conifer canopy with 95% forest cover. Snow depths and water equivalent are measured daily (except on weekends) and eight lysimeters record melt outflow each hour. The data from the open site used in this study were collected between November 14, 1985 and July 1, 1986 when the snowpack disappeared at the open site at a 6 hour time step. A total of 124 snow water equivalent measurements in addition to hourly lysimeter data were available for this time period. This dataset was used to test the new surface UEB model.

Niwot Ridge, Colorado

Another dataset used to test the new model comes from Subnivean snow laboratory at Niwot Ridge on the eastern slope of the Front Range of Colorado (3517 m MSL, $40^{o}03'$ N, $105^{o}35'$ W) collected during the 1995~1996 winter seasons. The instrument site is located in a relatively flat area above the treeline within a broad saddle of the ridge. The high elevation and exposure of Niwot Ridge, and typically dry atmospheric conditions, result in large clear-sky atmospheric transmissivity, high solar insolation, and low magnitudes of incident longwave radiation, low air temperatures, and high wind velocities. The dataset includes measurements of air temperature, wind speed, relative humidity, and incident shortwave radiation from April 28, 1996 to September 30, 1996 with a time step of 2 hours. Measured lysimeter data are also available although there are concerns as to how representative it is due to preferential flow paths (finger-flow) in the snow resulting in under-catch of meltwater (Cline, 1997a). The new surface UEB model was validated against this data for further variability research of the spatial distribution of snow water equivalent in the year of 1996.

5. Results

The new surface UEB model with the modified force-restore surface temperature parameterization was calibrated against the data from the USUDFto adjust some parameters and reflect the model changes. The model was then tested at the CSSL site. The model was validated using data from the Niwot ridge site, testing to some degree the physical basis and transferability of the model parameters.

At USUDF, Luce (2000) and Luce and Tarboton (2010) found evidence that the estimates of the incoming longwave radiation used in the original model testing (Tarboton *et al.*, 1995; Tarboton and Luce, 1996) were too low due to frequent inversions during winter. Luce (2000) estimated the downward longwave radiation flux from the total snowpack energy balance during non-melt periods given all other energy components such as ground heat flux, net shortwave radiation, turbulent fluxes and outgoing longwave radiation. The corrected longwave estimates were validated against cloud and fog observations at a nearby airport. In validating the new surface energy approximation, we used the measured shortwave radiation, the downward longwave radiation estimated by Luce (2000), and the measured ground heat flux to drive implementations of surface UEB with each of the three alternative surface temperature parameterizations given above (Equilibrium gradient, Force-restore and Modified Force-restore). The new surface model includes parameters from the original UEB model as well as new parameters introduced with the enhancements. Although there is some degree of circularity in using the total energy balance as an estimator of one stream of incoming energy, none of the alternative surface temperature parameterizations and none of the refreezing components were used in making the estimates. Consequently, comparisons among alternative model choices are nominally unaffected by the partially calibrated longwave radiation estimates at the USUDF location, and the results should be viewed in the context of a comparison for different approaches and incremental improvement rather than as a validation per se. Table 1 gives parameter values indicating which are new, and which were adjusted from their original UEB values to fit the data at USUDF as discussed below.

5.1 Modeled internal energy of snow

Figure 3 shows the time series of measured snow, ground and snow surface temperatures at the USU Drainage Farm that were used to calculate the internal energy content of the snowpack. Because this measured internal energy is only based on temperatures and does not account for any liquid water present, measured internal energy content is only comparable to modeled internal energy during cold periods when liquid water is not present. During warm periods, the modeled energy content is expected to go above zero while measured energy content remains close to (just below) zero. The three approaches for surface temperature approximation described above were included as options in the new surface UEB. (The original UEB model only had the gradient approach). The comparisons between the modeled and measured internal energy values (Figure 4) focus on periods when the snow is cold and liquid water is not present. These comparisons appear similar to the initial work of Luce (2000, Figure 2-5) and Luce and Tarboton (2001; 2010) that indicates that the modified force restore snow surface temperature approximation compares best to the internal energy content of snowpack. Here we note that these results differ from the earlier work of Luce (2000) and Luce and Tarboton (2001; 2010) in that the new results are complete model simulations driven by inputs of air temperature, humidity, radiation and wind with surface temperature calculated by the model. The earlier work used the measured surface temperature to drive calculations of internal energy estimating only the conduction into the snow, which does not test interactions of the new scheme with energy fluxes dependent on surface temperature. The results here are from a free running model forced by weather inputs that do test the modeling of dynamic interactions among the surface energy exchanges and surface temperature. Some parameters and physical properties quantified earlier (Luce and

Tarboton, 2001; 2010) were used here. Following the success of the modified force-restore surface temperature approach relative to the other approaches at the USUDF, the modified force-restore was used in all subsequent evaluations at the other sites.

Comparisons between modeled and measured variables at USUDF are shown in Figures 5, 6, 7, and 8. Figure 5 includes measured snow water equivalent and the results from five model runs. Four model runs are from the new surface UEB model using the parameters listed in table 1, each initialized on a different date indicated by the letters (a) through (d) following periods of severe weather and likely erroneous inputs. The fifth model run is from the original UEB model with its original parameters reported by Tarboton (1994). Figure 6 shows the measured and modeled energy content from the new surface UEB model run initialized on 1/26/1993 together with a model run using the code prior to the addition of the refreezing parameterization. Note that with the addition of the refreezing parameterization, lower energy content, better in line with measurements is obtained than without the refreezing parameterization.

Figure 7 shows measured and modeled energy content from the original UEB model, indicating a large discrepancy in energy content. This problem was identified by this comparison to internal energy computed from temperature profile measurements (Figure 3). This discrepancy has been resolved (Figure 6) through the combination of modifications reported in this paper (modified Force-Restore, surface refreezing and shallow snow conductivity adjustment). These results point to the importance of comparing models to measurements of their internal state as without the direct comparison to energy content the discrepancy with the original UEB may not have been identified.

5.2 Modeled snow water equivalent and meltwater

Figure 8 shows surface temperature comparisons for two time intervals chosen to be illustrative of periods prior to the onset of melt and during the period when snow is melting. The model runs shown in Figure 8 (a) were initialized on Jan. 26, 1993. The original UEB model run shown in Figure 8 (b) is the same as in Figure 8 (a) while the new surface UEB model run shown was initialized on Mar. 9, 1993. Note that these surface temperature comparisons, such as were used in the development of the original UEB do not indicate the energy discrepancy that full profile temperature measurements reveal.

The new surface UEB model and the calibrated model parameters were then tested using the 1985 -1986 data from the CSSL, CA. Comparisons of the modeled and the measured variables are shown in Figures 9, 10, 11, and 12. The modeled results well fit the measurements. More descriptions of the results were present in the discussion section.

The new surface UEB model was also tested using 1996 data from the Subnivean Snow Laboratory at Niwot Ridge, CO. Modeled and observed snow water equivalent are compared in Figure 13. The model was initialized with the beginning observed snow water equivalent value of 1.4 m. Melt outflows that totaled to 0.23 m were recorded. These were used to infer the snow water equivalent back through time. However, as shown in Figure 13, there is a discrepancy between the measured total melt (0.23 m) and observed initial snow water equivalent (1.4 m). This is presumed to be due to preferential meltwater drainage flow paths in the snow as reported previously at this location (Cline, 1997b). An adjustment factor was calculated as $\frac{W_{ini} + \sum p}{\sum m}$, where W_{ini} is the initial measured snow water equivalent, $\sum p$ is the total precipitation during the modeling time, and $\sum m$ is the total measured meltwater outflow.

5.3 Modeled albedo

The USUDF instrumentation included a net radiometer and downward and upward pointing pyranometers. These were used to obtain a measured estimate of Albedo that was compared to albedo as simulated by the original model and new surface UEB model (Figure 14). These results indicated that albedo was not being refreshed to new snow values following snowfall. This was corrected by changing the threshold of new snow water equivalent that restores albedo to the new snow cover, d_{NewS}, to 0.002 m; this was previously 0.01 m.

6. Discussion

The most significant change introduced into the surface UEB model was the change to the surface temperature parameterization. Figure 9 shows the snow water equivalent data originally used to validate the UEB model, together with surface temperature comparisons, such as Figure 8 and melt outflow comparisons such as Figure 10. These results looked satisfactory at the time, but once measurements of internal energy (Figure 7) were obtained it was realized that the original UEB had problems representing internal energy and this deficiency was traced in part to the surface temperature parameterization (Luce and Tarboton 2010). Incorporating the modified force restore approach they suggested into the UEB model resulted in improvements in snowpack internal energy estimates (Figure 4).

Density and thermal conductivity are the primary parameters introduced in the new parameterization of surface temperature (equations 21, 22 and 23). Variability in thermal conductivity as a function of snow density is to be expected as both are determined by the snow's microstructure but are not uniquely related to each other. Measurements of the thermal conductivity of snow are thoroughly reviewed by Sturm et al. (1997). In the literature there is variability in the values reported for thermal conductivity (Anderson, 1976; Gray and Male, 1981; Lee, 1980). Anderson (1976, p30 Figure 3.1) shows that the thermal conductivity of the snowpack may change over a wide range from 0.15 kJ m^{-1} h^{-1} K^{-1} to 7.5 kJ m^{-1} h^{-1} K^{-1} at a density of 200 kg m^{-3}. Lee (1980) also reported a range from 0.25 kJ m^{-1} h^{-1} K^{-1} at a density of 100 kg m^{-3} to 5.3 kJ m^{-1} h^{-1} K^{-1} at a density of 700 kg m^{-3}. Gray and Male (1981) indicated that thermal conductivity changes are nonlinear from 0.18 kJ m^{-1} h^{-1} K^{-1} at a density of about 175 kg m^{-3} to 5.76 kJ m^{-1} h^{-1} K^{-1} at a density of 800 kg m^{-3}. The UEB model retains a degree of simplicity by not modeling surface density and thermal conductivity as time varying quantities. The surface UEB uses a single thermal conductivity value and snow density, and the values of λ_s = 0.33 kJ m^{-1} h^{-1} K^{-1} and ρ_s = 200 kg m^{-3} were calibrated to fit the internal energy measurements of Figure 4 considering the snow thermal properties inferred from frequency analysis by Luce and Tarboton (2010). Snow density is reflective of the density of the snow surface, involved in surface energy exchanges, rather than the snowpack as a whole. Modeling the thermal conductivity as a function of density may improve the performance of snowmelt models if the density was able to be apporprietely modeled. However, the errors in modeling the density may also brought in errors in modeling the surface heat conduction and the internal energy content.

A value of r=1 was used for the dimensionless damping depth factor. This nominal value corresponds to a gradient over the depth to which diurnal temperature fluctuations are attenuated by a factor of 1/e. The soil thermal conductivity parameter also plays a role in the model when the snowpack is shallow (Equation 40) and was set to a value of 6.5 kJ m^{-1} h^{-1} K^{-1}, within the range of soil heat conductivity reported for the Logan Area (Hanks and Ashcroft, 1980; Luce, 2000). The low frequency forcing frequency value, w_{lf}, was set to 0.0654 rad/h based on Luce and Tarboton (2010).

It is interesting to note that with a new surface temperature parameterization calibrated to USUDF data, the model better represents the CSSL snow water equivalent data (Figure 9) and cumulative melt data (Figure 10) early in the season. This model successfully resolves the failure to capture early-season melt, a problem which is a fairly common feature of single-layer models (Slater et al. 2001). The model now holds energy content closer to zero and is able to represent early season melt, correcting the relatively small early season discrepancy in comparisons to CSSL data that was present in the original UEB model calibrations. Small discrepancies still exist in the modeled snow water equivalent and the measurement snow water equivalent at the high accumulation period. This may be due to remaining model errors and some uncertainty (undercatch) in the snowfall measurements that are inputs. The disappearance date of the snow at CSSL was still modeled about one week later than the observed, which may be due to errors in modeling the decrease of albedo perhaps due to contamination of the snow or due to the increase of longwave radiation from the nearby forest canopy.

Representation of observed snow water equivalent at USUDF in a single model run proved to be difficult. We attributed this to uncertainty and likely erroneous input quantities during windy and stormy severe weather periods. Snowfall was recorded in a heated unshielded precipitation gauge so is uncertain and likely to suffer from undercatch.

There was also snow drifting resulting in accumulation and scour associated with strong winds, and griming of the instruments recording radiation.

One of the problems discovered with the original UEB model was that it offsets the bias due to the surface temperature parameterization by a bias in heat loss following surface melting (Figure 6). Following a period of snowmelt, the observed energy content is observed to fall below 0 but the modeled energy content remained above 0. Without the refreezing parameterization surface temperature immediately drops in a cooling period, limiting the heat loss by reducing the outgoing longwave radiation. The parameterization of the refreezing front corrected this to some extent (Figure 6) keeping the surface temperature warmer and sustaining greater outgoing longwave radiation energy losses, the extra energy loss going to refreeze liquid water present and allowing the model energy content to drop more in line with the observations.

Melt outflow rates were not measured at USUDF. The changes in surface temperature and refreezing parameterization changed the modeled amount of liquid water, which changed melt outflow. We used measured melt outflow at CSSL (Figure 11) to adjust the snow hydraulic conductivity to 200 m h^{-1}, a value still within the range from 20 m h^{-1} to 300 m h^{-1} reported in the literature (Gray and Male, 1981). Liquid holding capacity was adjusted to 0.02 to better fit melt outflow.

D_e and z_0 were adjusted based on the research of Luce (2000) and Luce and Tartboton (2010) where a value of 0.1 m was suggested for the soil effective depth and a value 0.01 m suggested for the surface aerodynamic roughness of snow z_0 in the calculation of turbulent heat flux.

The Albedo measurements at USUDF enabled refinement of the parameter quantifying the new snow water equivalent that restores albedo to the new snow cover, resulting in a more responsive modeling of albedo, consistent with observations (Figure 14). However, there is an offset between modeled and observed albedo in this figure, which, we believe, is due to downward pointing limited-band pyranometers not being appropriate for measuring snow reflectance. However they do still provide us with relative measurements useful in quantifying the timing and responsiveness of albedo changes.

As was observed at the USU drainage farm, the new surface model also gave a good approximation of the surface temperature of snow (Figure 12) at the CSSL snow laboratory. Both the new model and the original model perform well in approximating the surface temperature of snow at CSSL site. However, the new model corrects the offsets between the modeling of snow surface temperature and the modeling of the internal energy of the snowpack in the original model. Here we note that uncertainties exist in the measurements, e.g., the measurement of surface temperature of snow has positive value during some daytime periods.

The comparison between modeled and measured snow water equivalent at Niwot Ridge inferred from observed initial snow water equivalent and melt outflow is given in Figure 13. This shows that after the adjustment to correct the discrepancy between initial snow water equivalent and measured melt, the back-calculated snow water equivalent compares well with modeled snow water equivalent. Due to the adjustment involved this is really only a check on the timing of the ablation.

7. Conclusions

This paper has: (1) Evaluated the force restore and modified force restore temperature parameterizations developed for a single layer snowmelt model in a complete energy balance free-running model driven by only atmospheric forcing; (2) Introduced and evaluated a new parameterization for the refreezing of liquid water near the surface in an energy balance snowmelt model; and (3) Introduced a refinement to adjust thermal conductivity parameters for shallow snowpacks. Collectively these contributions have solved the issue of overestimating the energy loss of snowpack and underestimating the average snow temperature in an earlier version of the UEB snowmelt model. With these refinements, the model was better able to represent internal energy content, snow surface temperature, early and late season snowmelt and albedo quite well. Through this modeling work the understanding of snow surface energy exchanges and how they can be more effectively modeled has improved.

This work has integrated information from a number of measurement sources to validate and improve parameterization of processes in the model. Without the temperature profile measurements that quantified internal energy, the energy content discrepancy would have been hard to identify.

The new surface UEB snowmelt model has been calibrated and tested against datasets from the USU Drainage Farm and CSSL snow laboratory and performed well at these two sites. The paper also included tests against some data from Niwot ridge, Colorado. However some discrepancies still exist between the modeled variables and the observations. Also some variables cannot be strictly compared or compared against a complete dataset. A more complete dataset of the liquid water content, together with continuous observation of snow water equivalent, snow surface temperature, melt, and depth, is necessary for a comprehensive test of the model improvements given here. This speaks to the need for integrated measurements of multiple variables at each of multiple sites to more fully constrain snow mass and energy processes to further improve snow models. Such datasets are becoming available (Morin *et al*., 2012) and it is important for future studies to take advantage of such datasets, and for more of such datasets to be collected.

Surface UEB is a single layer model designed to be parsimonious, yet use physically based calculations for the energy and mass exchanges at the snow surface so as to be transferable, with limited calibration, to other locations. This transferability was evaluated to a limited extent in this paper by using multiple somewhat geographically dispersed test sites in Utah, Colorado and California. The results thus provide some level of confidence in the transferability of the model, though further testing at additional sites would add to the confidence in the model transferability, or lead to further improvements. Surface UEB uses a limited number of state variables so as to be easy to apply in a spatially distributed fashion. It focuses on surface energy exchanges and surface temperature as the variable at the interface between the surface and atmosphere governing energy exchanges. It avoids attempting to represent the internal energy exchanges between snowpack layers thereby avoiding the introduction of errors due to the challenges in representing these complex internal snow processes. UEB compared favorably against more complex layered models in a recent model intercomparison (Rutter et al., 2009). Further evaluation of surface UEB together with other models in different climate and topographic settings, as suggested in Rutter et al. (2009), should be pursued.

Acknowledgments

This work was supported by NASA Land Surface Hydrology Program, grant number NAG 5-7597. The views and conclusions expressed are those of the authors and should not be interpreted as necessarily representing official policies, either expressed or implied, of the U.S. Government.

References

Anderson, E. A.: A Point Energy and Mass Balance Model of a Snow Cover. NOAA Technical Report NWS 19, U.S. Department of Commerce. 150 pp. 1976.

Berg, P. W, and McGregor, J. L.: *Elementary Partial Differential Equations*. Holden-Day: Oakland. 1966.

Blöschl, G., and Kirnbauer, R.: Point snowmelt models with different degrees of complexity - internal processes. *Journal of Hydrology* **129**: 127-147. 1991.

Bras, R. L.: *Hydrology, an Introduction to Hydrologic Science*. Addison-Wesley: Reading, MA. 1990.

Bristow, K. L, and Campbell, G. S.: On the relationship between incoming solar radiation and the daily maximum and minimum temperature. *Agricultural and Forest Meteorology* **31**: 159-166. 1984.

Cline, D. W.: Snow surface energy exchanges and snowmelt at a continental, midlatitude alpine site. *Water Resources Research* **33**(4): 689-701. 1997a.

Cline, D. W.: Effect of seasonality of snow accumulation and melt on snow surface energy exchanges at a continental alpine site. *Journal of Applied Meteorology* **36**: 22-41. 1997b.

Colbeck, S. C.: Air movement in snow due to windpumping. *Journal of Glaciology* **35**(120): 209-213. 1989.

Colbeck, S. C, and Anderson, E. A.: The Permeability of a Melting Snow Cover. *Water Resources Research* **18**(4): 904-908. 1982.

Deardorff, J.W.: Dependence of Air-Sea Transfer Coefficients on Bulk Stability. *Journal of Geophysical Research* **73**(8): 2549-2557. 1968.

Deardorff, J. W.: Efficient prediction of ground surface temperature and moisture with inclusion of a layer of vegetation. *Journal of Geophysical Research* **83**: 1889-1903. 1978.

Dickinson, R. E, Henderson-Sellers, A., and Kennedy, P. J.: Biosphere-Atmosphere Transfer Scheme (BATS) Version 1e as Coupled to the NCAR Community Climate Model. NCAR/TN-387+STR, National Center for Atmospheric Research. Boulder, CO; 71 pp. 1993.

Dingman, S. L.: *Physical Hydrology*. Macmillan: New York. 1994.

Dozier, J. Spectral Signature of Alpine Snow Cover from the Landsat Thematic Mapper. *Remote Sensing of Environment* **28**: 9-22. 1989.

Dyer, A. J., and Hicks, B. B.: Flux-gradient Relationships in the Constant Flux Layer. *Quart. J. R. Met. Soc.* **96**: 715-721. 1970.

Eiriksson, D., Whitson, M., Luce, C. H., Marshall, H. P., Bradford, J., Benner, S. G., Black, T., Hetrick, H., and McNamara, J. P.: An evaluation of the hydrologic relevance of lateral flow in snow at hillslope and catchment scales, Hydrological Processes, 27, 640-654, 10.1002/hyp.9666, 2013.

Flerchinger, G. N, and Saxton, K. E.: Simultaneous Heat and Water Model of a Freezing Snow-Residual- Soil System I. Theory and Development. *Transactions of the ASAE* **32**(2): 565-571. 1989.

Gray, D. M., and Male, D. H. (eds): Handbook of Snow, Principles, Processes, Management & Use. Pergamon Press: New York. 1981.

Hanks, R. J, and Ashcroft, G. L.: *Applied Soil Physics*. Vol 8, Advanced Series in Agricultural Sciences, Springer-Verlag: Berlin Heidelberg. 1980.

Higuchi, K., and Tanaka, Y.: Flow pattern of meltwater in mountain snow cover, Hydrological aspects of alpine and high-mountain areas, Hydrological Sciences Journal, 27, p 256, 1982.

Hu, Z., and Islam, S.: Prediction of ground surface temperature and soil moisture content by the force-restore method. *Water Resources Research* **31**(10): 2531-2539. 1995.

Jin, J., Gao, X., Sorooshian, S., Yang, Z-L., Bales, R., Dickinson, R. E., Sun, S-F., and Wu, G-X.: One-dimensional snow water and energy balance model for vegetated surfaces. *Hydrological Processes* **13**: 2467-2482. 1999.

Jordan, R.: A One-dimensional Temperature Model for a Snow Cover. Technical documentation for SNTHERM.89, special technical report 91-16, US Army CRREL. 49 pp. 1991.

Kattelmann R, Dozier J. Observations of snowpack ripening in the Sierra Nevada, California, USA. Journal of Glaciology 45: 409–416, 1999.

Koivasulo, H., and Heikenkeimo, M.: Surface energy exchange over a boreal snowpack. *Hydrological processes* **13**(14/15): 2395-2408. 1999.

Lee, R.: *Forest Hydrology*. Columbia University Press: New York. 1980.

Linsley, R. K, Kohler, M. A., and Paulhus, J. L. H.: *Hydrology for Engineers*. 2nd Edition, McGraw-Hill: Kogakusha, Ltd. 1975.

Lowe, P. R.: An approximating polynomial for the computation of saturation vapour pressure. *Journal of Applied Meteorology* **16**: 100-103. 1977.

Luce, C. H.: Scale influences on the representation of snowpack processes. Ph. D Dissertation, Civil and Environmental Engineering: Utah State University, Logan, Utah. 2000.

Luce, C. H, and Tarboton, D. G.: A modified force-restore approach to modeling snow-surface heat fluxes. In *Proceedings of the 69th Annual Meeting of the Western Snow Conference,* Sun Valley, Idaho. http://www.westernsnowconference.org/2001/2001papers.htm. (Accessed Jul. 31, 2004). 2001.

Luce, C. H, Tarboton, D. G., and Cooley, K. R.: The influence of the spatial distribution of snow on basin-averaged snowmelt. *Hydrological Processes* **12**(10-11): 1671-1683. 1998.

Luce, C. H., and Tarboton, D. G.: Evaluation of alternative formulae for calculation of surface temperature in snowmelt models using frequency analysis of temperature observations, *Hydrol. Earth Syst. Sci*., 14, 535-543, 2010.

Mahat, V., and Tarboton, D. G.: Canopy radiation transmission for an energy balance snowmelt model, Water Resour. Res., 48: W01534, http://dx.doi.org/10.1029/2011WR010438. 2012.

Mahat, V., Tarboton, D. G., and Molotch, N. P.: Testing above and below canopy representations of turbulent fluxes in an energy balance snowmelt model, Water Resources Research, in press, http://dx.doi.org/10.1002/wrcr.20073. 2013.

Marks, D., Kimball, J., Tingey, D., and Link, T.: The sensitivity of snowmelt processes to climate conditions and forest cover during rain-on-snow: a case study of the 1996 Pacific Northwest flood. *Hydrological Processes* **12**(10-11): 1569-1598. 1998.

Prasad, R., Tarboton, D. G., Liston, G. E., and Luce, C. H., Seyfried, M. S.: Testing a blowing snow model against distributed snow measurements at Upper Sheep Creek. *Water Resources Research* **37**(5): 1341-1350. 2000.

Price, A. G., and Dunne, T.: Energy balance computations of snowmelt in a subarctic area. *Water Resources Research* **12**(4): 686-694. 1976.

Rutter, N., Essery, R., Pomeroy, J., Altimir, N., Andreadis, K., Baker, I., Barr, A., Bartlett, P., Boone, A., Deng, H., Douville, H., Dutra, E., Elder, K., Ellis, C., Feng, X., Gelfan, A., Goodbody, A., Gusev, Y., Gustafsson, D., Hellström, R., Hirabayashi, Y., Hirota, T., Jonas, T., Koren, V., Kuragina, A., Lettenmaier, D., Li, W.-P., Luce, C., Martin, E., Nasonova, O., Pumpanen, J., Pyles, R. D., Samuelsson, P., Sandells, M., Schädler, G., Shmakin, A., Smirnova, T. G., Stähli, M., Stöckli, R., Strasser, U., Su, H., Suzuki, K., Takata, K., Tanaka, K., Thompson, E., Vesala, T., Viterbo, P., Wiltshire, A., Xia, K., Xue, Y., and Yamazaki, T.: Evaluation of forest snow processes models (snowmip2), J. Geophys. Res., 114, D06111, 2009.

Satterlund, D. R.: An improved equation for estimating long-wave radiation from the atmosphere. *Water Resources Research* **15**: 1643-1650. 1979.

Slater, A. G., Schlosser, C. A., Desborough, C. E., Pitman, A. J., Henderson-Sellers, A., Robock, A., Vinnikov, K. Y., Entin, J., Mitchell, K., Chen, F., Boone, A., Etchevers, P., Habets, F., Noilhan, J., Braden, H., Cox, P. M., de Rosnay, P., Dickinson, R. E., Yang, Z. L., Dai, Y. J., Zeng, Q., Duan, Q., Koren, V., Schaake, S., Gedney, N., Gusev, Y. M., Nasonova, O. N., Kim, J., Kowalczyk, E. A., Shmakin, A. B., Smirnova, T. G., Verseghy, D., Wetzel, P., and Xue, Y.: The representation of snow in land surface schemes: Results from PILPS 2(d), Journal of Hydrometeorology, 2, 7-25, 10.1175/1525-7541(2001)002<0007:trosil>2.0.co;2, 2001.

Sturm, M., Holmgren, J., König, M., and Morris, K.: The thermal conductivity of seasonal snow. *J. Glaciol.*, **43**, 26 – 41. 1997.

Sun, S., Jin, J., and Xue, Y.: A simple snow-atmosphere-soil transfer model. *Journal of Geophysical Research* **104**(D16): 19587-19597. 1999.

Tarboton, D. G.: Measurement and modeling of snow energy balance and sublimation from snow. In *Proceedings of International Snow Science Workshop*, Snowbird, Utah, October 31 to November 2; 260-279. 1994.

Tarboton, D. G., Chowdhury, T. G., and Jackson, T. H.: A spatially distributed energy balance snowmelt model. In *Proceedings of a Boulder Symposium*, Tonnessen KA, Williams MW, Tranter M (eds). Boulder, CO., July 3-14, IAHS Publ. no. 228. 1995.

Tarboton, D. G., and Luce, C. H.: Utah Energy Balance Snow Accumulation and Melt Model (UEB). Computer model technical description and users guide, Utah Water Research Laboratory and USDA Forest Service Intermountain Research Station (http://www.engineering.usu.edu/dtarb/). (Accessed Jul. 31, 2004). 1996.

U.S. Army Corps of Engineers.: Snow Hydrology, Summary Report of the Snow Investigations. U.S. Army Corps of Engineers, North Pacific Division, Portland, Oregon. 142 pp. 1956.

Viessman, W., Lewis, G. L, and Knapp, J. W.: *Introduction to Hydrology*. 5th Edition, Prentice Hall: New York. 2002.

Vionnet, V., Brun, E., Morin, S., Boone, A., Faroux, S., Le Moigne, P., Martin, E., and Willemet, J. M.: The detailed snowpack scheme crocus and its implementation in surfex v7.2, Geosci. Model Dev., 5, 773-791, 10.5194/gmd-5-773-2012, 2012.

Wankiewicz, A.: A review of water movement in snow, in: Proceedings: Modeling of snow cover runoff, edited by: Colbeck, S. C., and Ray, M., U.S Army Cold Regions Research and Engineering Laboratory, Hanover, New Hampshire, 1979.

Warren, S. G.: Optical properties of snow. *Review of Geophysics* **20**: 67-89. 1982.

Wever, N., Fierz, C., Mitterer, C., Hirashima, H., and Lehning, M.: Solving richards equation for snow improves snowpack meltwater runoff estimations in detailed multi-layer snowpack model, The Cryosphere, 8, 257-274, 10.5194/tc-8-257-2014, 2014.

Williams, M. W., Erickson, T. A., and Petrzelka, J. L.: Visualizing meltwater flow through snow at the centimetre-to-metre scale using a snow guillotine, Hydrological Processes, 24, 2098-2110, 10.1002/hyp.7630, 2010.

Yen, Y.C.: The rate of temperature propagation in moist porous mediums with particular reference to snow. *Journal of Geophysical Research* **72** (4): 1283-1288. 1967.

You, J.: Snow hydrology: The parameterization of subgrid processes within a physically based snow energy and mass balance model, PhD thesis, Utah State Univ., Logan. 2004

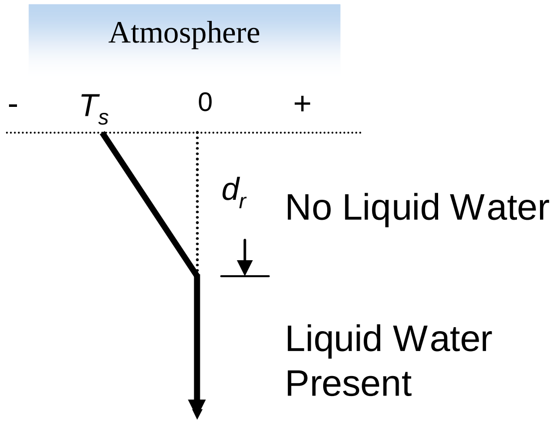

Figure 1 Schematic illustration of temperature profile during the downward propagation of a refreezing front.

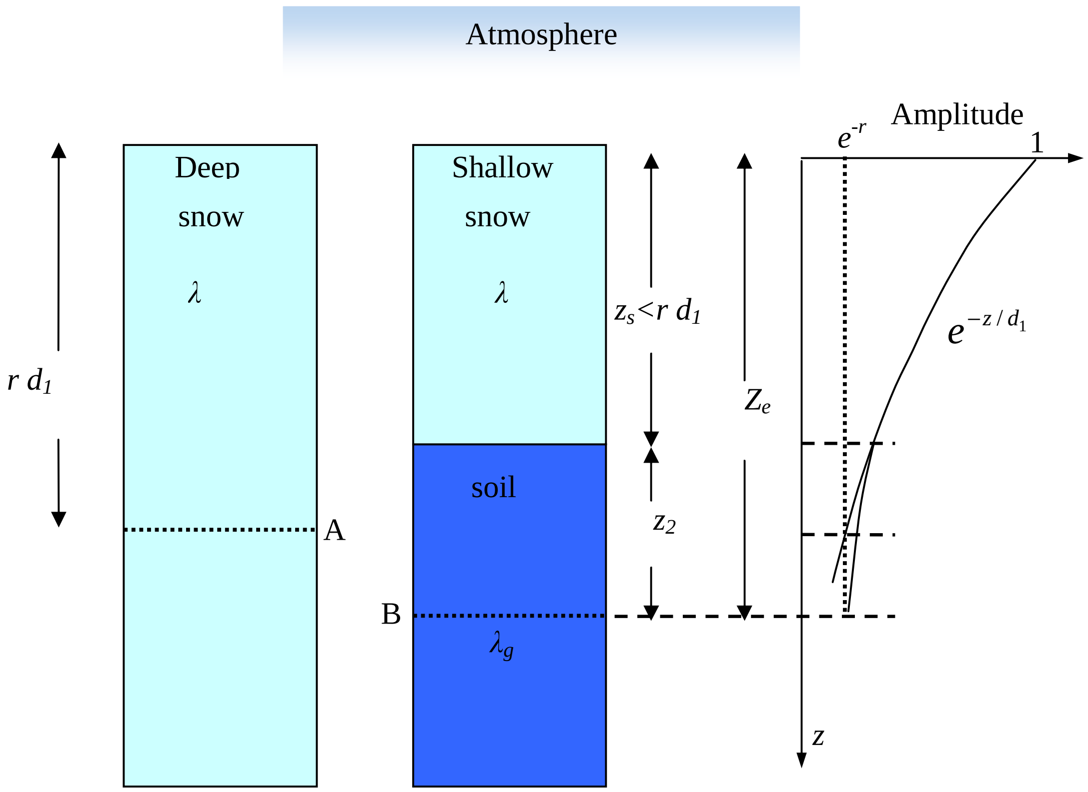

Figure 2 Heat conduction scheme for combined snow/soil system. The dashed lines at depths A and B indicate the depths at which temperature fluctuation amplitude is damped by e^{-r} in the deep snow and combined snow/soil system respectively.

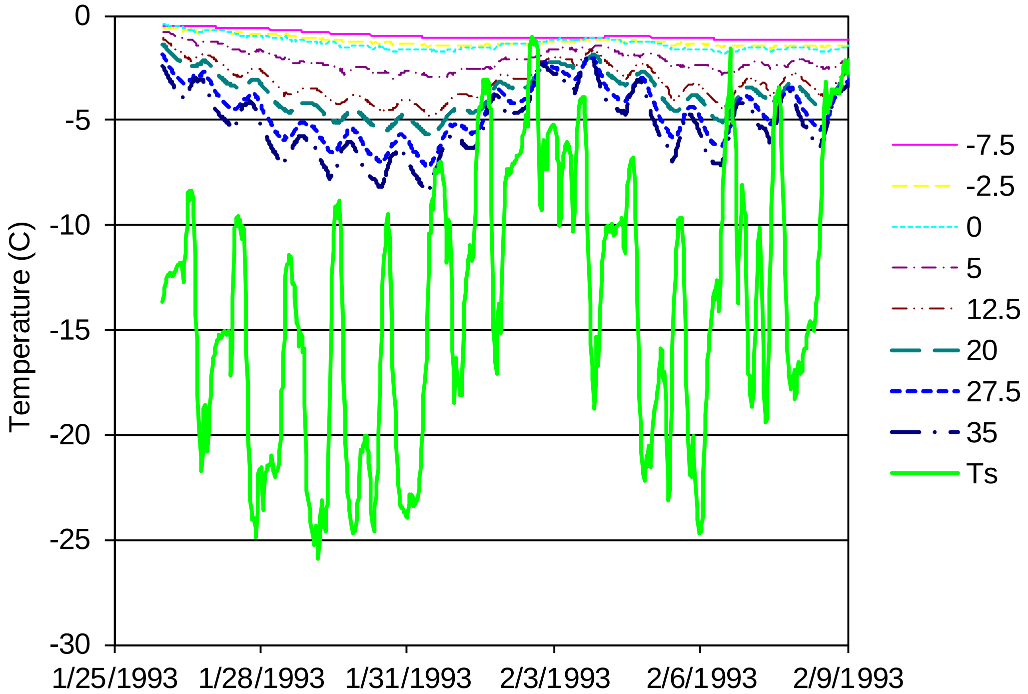

Figure 3 Measured snow, ground, and snow surface temperatures at the USU Drainage Farm. T_s is the measured surface temperature of snow from an infrared sensor. Other temperatures are from thermocouples labeled according to their height relative to the ground surface. Negative heights are below the ground surface and positive heights above the ground surface. 0 refers to the measured temperature at the ground surface.

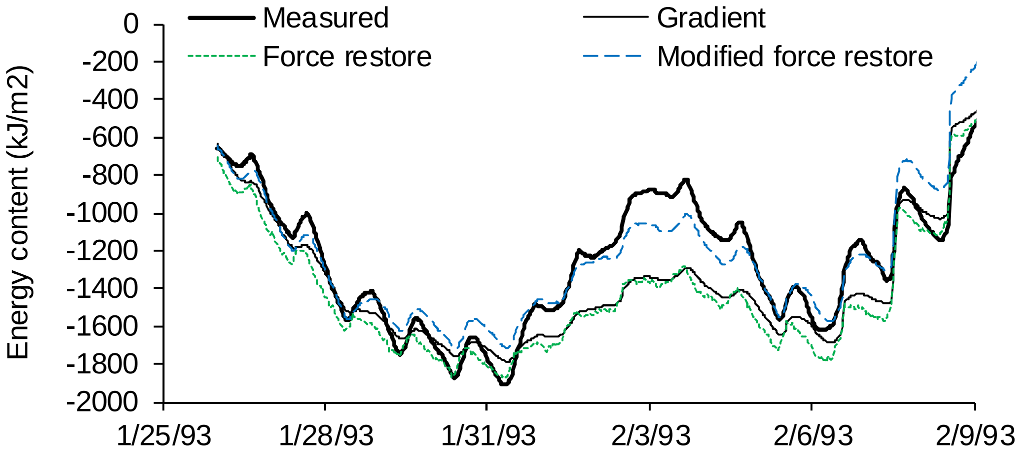

Figure 4 Comparisons of internal energy of snowpack during the first two freezing weeks at the USU Drainage Farm. Measured is the internal energy of snowpack calculated from the temperature profile (Figure 3). Gradient, Force restore, and Modified force restore represent the modeled internal energy of snowpack using the equilibrium approach, the force-restore approach, and the modified force restore approach respectively.

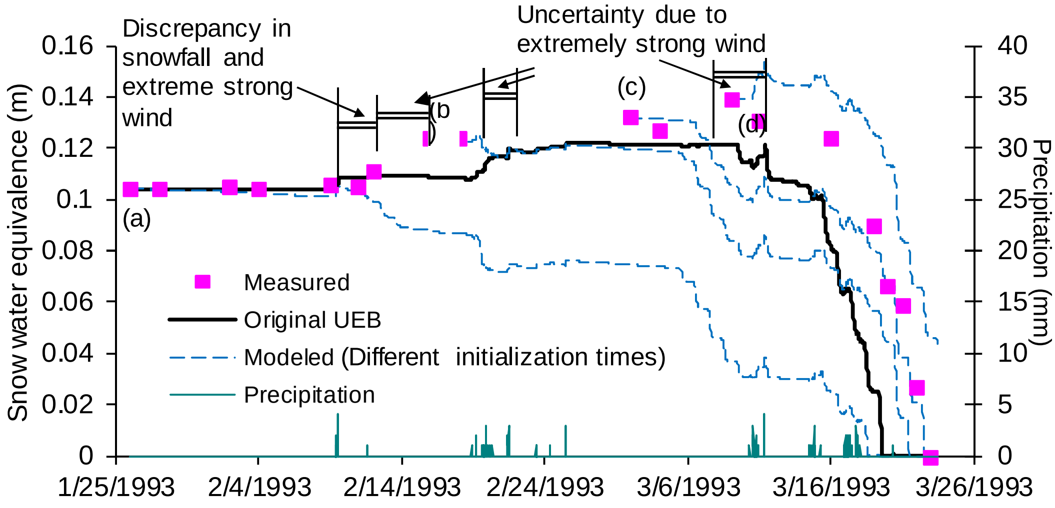

Figure 5 Comparisons of snow water equivalent in 1993 at the USU Drainage Farm. The dashed lines are the modeled values with new model starts at different times. Precipitation input is shown (spiky line at the bottom) relative to the axis at the right. Letters (a) through (d) indicate points where the model was re-initialized following periods of likely erroneous inputs due to severe weather.

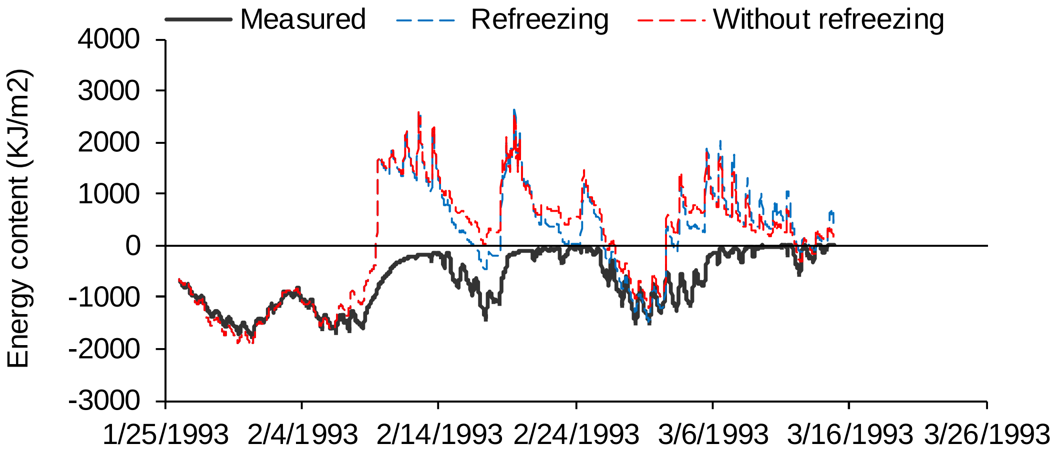

Figure 6 Comparisons of internal energy of snowpack in 1993 at the USU Drainage Farm. The wide solid line is the measured values. “Refreezing” represents the modeled internal energy of snowpack with new surface UEB model. “Without refreezing” represents the model without the refreezing scheme.

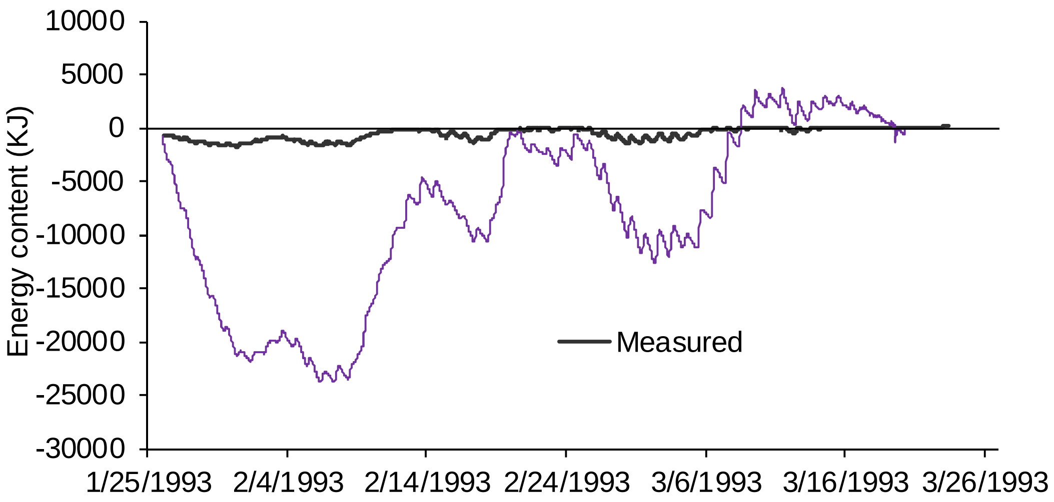

Figure 7 Comparisons between the measured and modeled internal energy of the snowpack at the USU Drainage Farm in the original model.

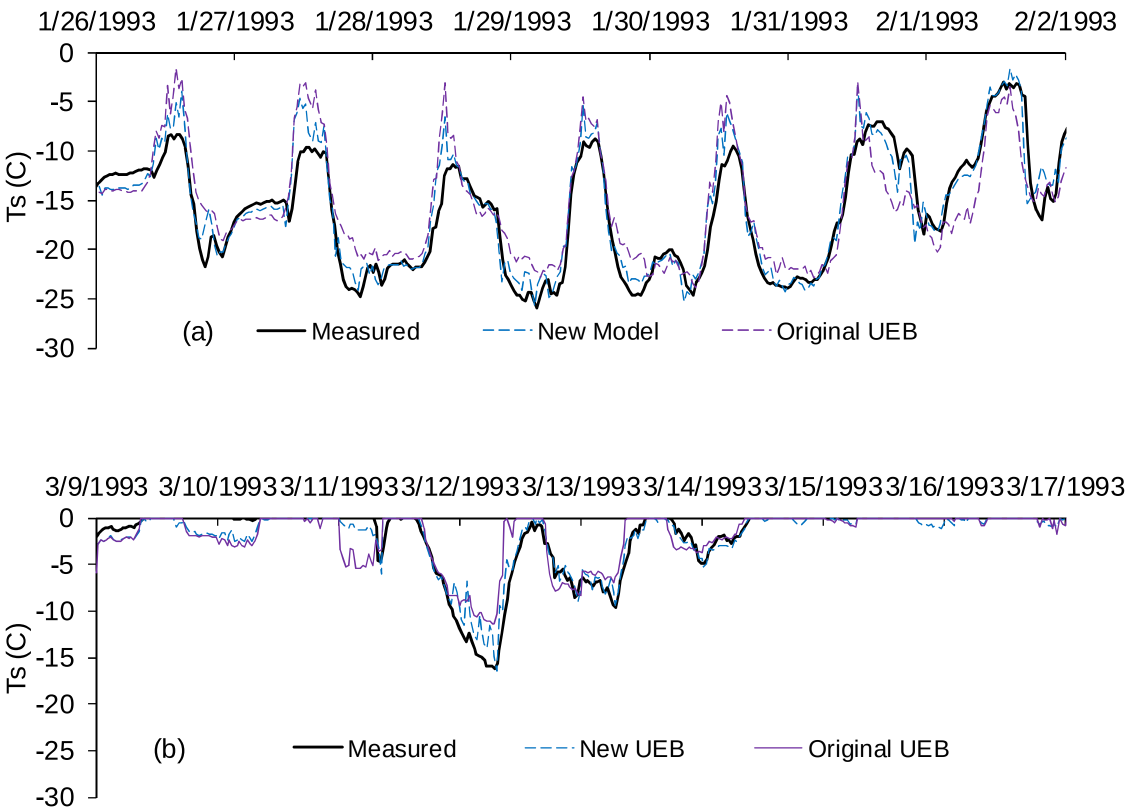

Figure 8 Comparisons of snow surface temperature in 1993 at the USU Drainage Farm. (a) the first two subfreezing weeks, and (b) end of the modeling period when the snowpack is occasionally in an isothermal state.

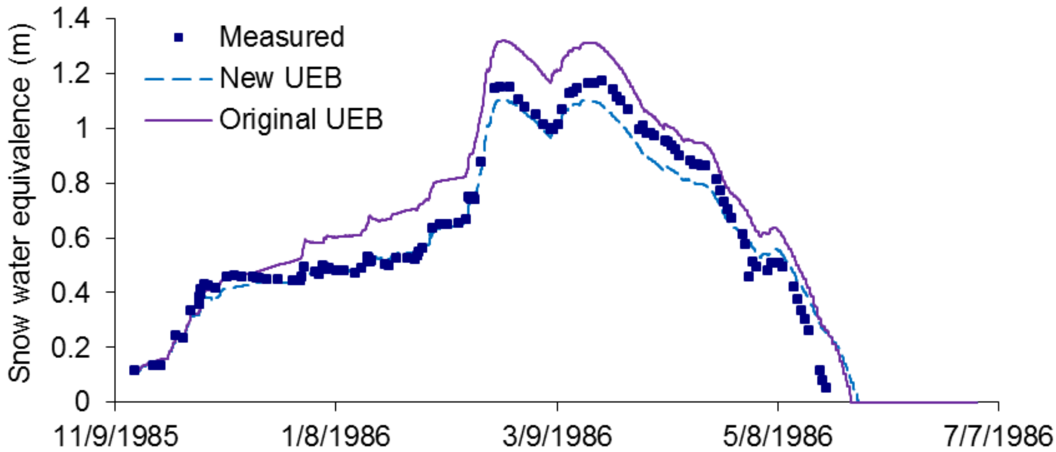

Figure 9 Comparisons of snow water equivalent in 1986 at CSSL.

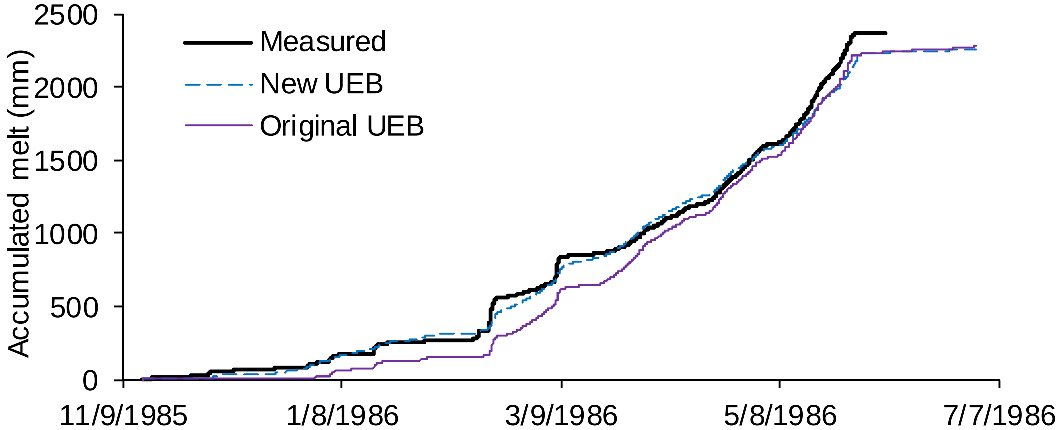

Figure 10 Comparisons of accumulative melt in 1986 at CSSL.

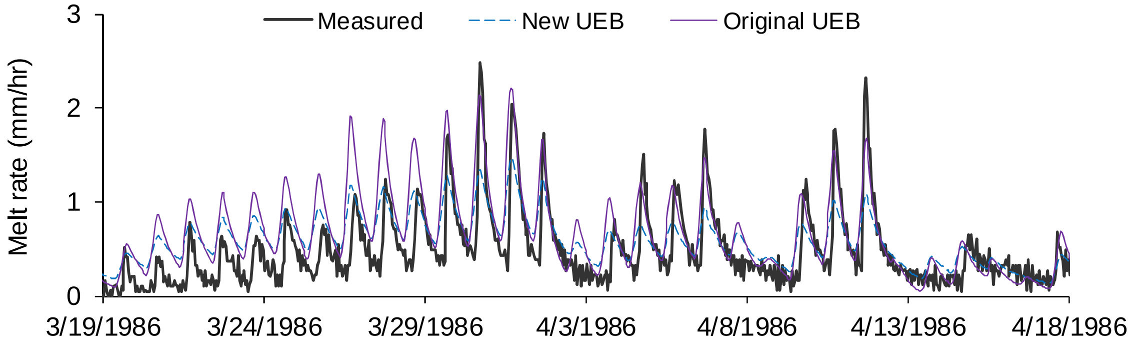

Figure 11 Comparisons of meltwater outflow rate in 1986 at CSSL

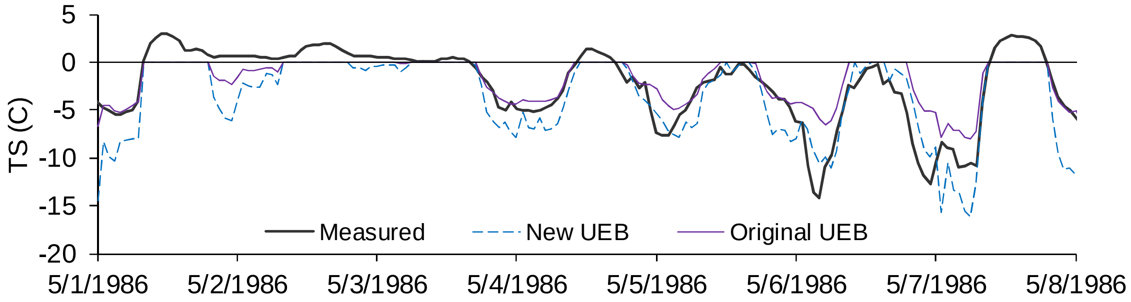

Figure 12 Comparisons of surface temperature of snow in 1986 at CSSL

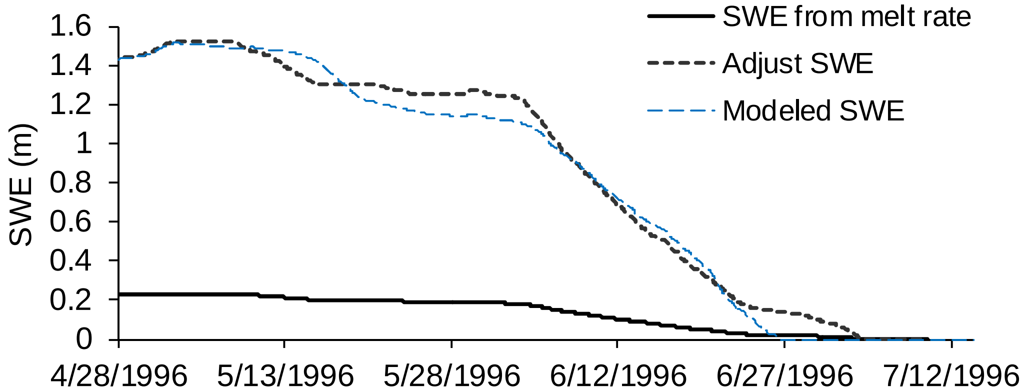

Figure 13 Comparisons of snow water equivalent in 1996 at Subnivean Snow Laboratory at Niwot Ridge watershed, CO.

1173

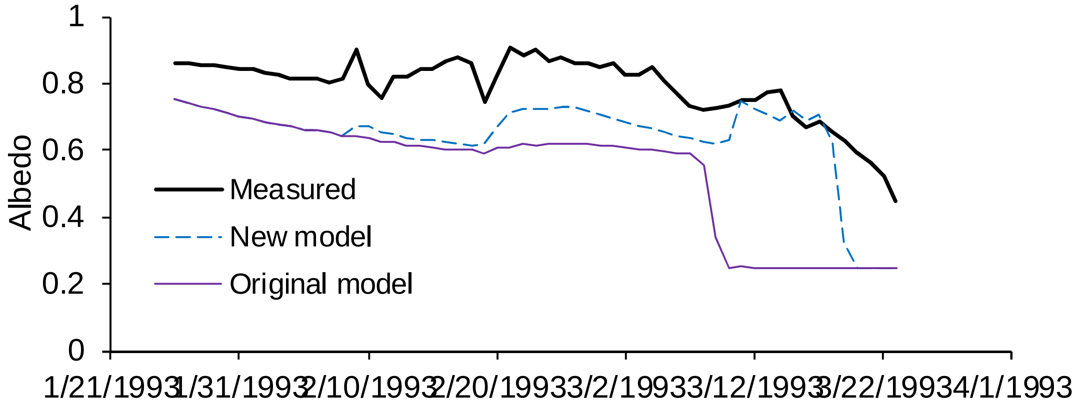

1174

1175 Figure 14 Comparison of measured and modeled albedo at the USU drainage farm.

1176

1177

Table 1 Model parameter values

Parameters	Value
Thermal conductivity of snow λ_s	**0.33 kJ m^{-1} K^{-1} h^{-1}
Thermal conductivity of soil λ_g	**6.5 kJ m^{-1} K^{-1} h^{-1}
Low frequency forcing frequency ω_{lf}	**0.0654 radians h^{-1} (ω_1/4)
Dimensionless damping depth factor r	**1
Threshold depth for fresh snow d_{NewS}	**0.002 m
Saturated hydraulic conductivity K_{sat}	*200 m h^{-1}
Surface aerodynamic roughness z_o	*0.01 m
Capillary retention fraction L_c	*0.02
Soil effective depth D_e	*0.1 m
Snow density ρ_s	*200 kg m^{-3}
Ground heat capacity C_g	2.09 kJ kg^{-1} K^{-1}
Density of soil layer ρ_g	1700 kg m^{-3}
Emissivity of snow ε_s	0.99
Temperature above which precipitation is rain T_r	3°C
Temperature below which precipitation is snow T_{sn}	-1 °C
Wind/air temperature measurement height z_m	2 m
Bare ground albedo α_{bg}	0.25
New snow near infrared band reflectance α_{iro}	65%
New snow visible band reflectance α_{vo}	85%

** These parameters are new, i.e., they were not present in the Original UEB

* These parameters were calibrated to have new values.

LIST OF TABLES

LIST OF FIGURES

Figure 1 Schematic illustration of temperature profile during the downward propagation of a refreezing front.

Figure 2 Heat conduction scheme for combined snow/soil system. The dashed lines at depths A and B indicate the depths at which temperature fluctuation amplitude is damped by e^{-r} in the deep snow and combined snow/soil system respectively.

Figure 3 Measured snow, ground, and snow surface temperatures at USU Drainage Farm. T_s is the measured surface temperature of snow from an infrared sensor. Other temperatures are from thermocouples labeled according to their height relative to the ground surface. Negative heights are below the ground surface and positive heights above the ground surface. 0 refers to the measured temperature at the ground surface.

Figure 4 Comparisons of internal energy of snowpack during the first two freezing weeks at the USU Drainage Farm. Measured is the internal energy of snowpack calculated from the temperature profile (Figure 3). Gradient, Force restore, and Modified force restore represent the modeled internal energy of snowpack using the equilibrium approach, the force-restore approach, and the modified force restore approach respectively.

Figure 5 Comparisons of snow water equivalent in 1993 at the USU Drainage Farm. The dashed lines are the modeled values with new model starts at different times. Precipitation input is shown (spiky line at the bottom) relative to the axis at the right. Letters (a) through

(d) indicate points where the model was re-initialized following periods of likely erroneous inputs due to severe weather.

Figure 6 Comparisons of internal energy of snowpack in 1993 at the USU Drainage Farm. The wide solid line is the measured values. "Refreezing" represents the modeled internal energy of snowpack with new surface UEB model. "Without refreezing" represents the model without the refreezing scheme.

Figure 7 Comparisons between the measured and modeled internal energy of the snowpack at the USU Drainage Farm in the original model.

Figure 8 Comparisons of snow surface temperature in 1993 at the USU Drainage Farm. (a) the first two subfreezing weeks, and (b) end of the modeling period when the snowpack is occasionally in an isothermal state.

Figure 9 Comparisons of snow water equivalent in 1986 at CSSL.

Figure 10 Comparisons of accumulative melt in 1986 at CSSL.

Figure 11 Comparisons of meltwater outflow rate in 1986 at CSSL

Figure 12 Comparisons of surface temperature of snow in 1986 at CSSL

Figure 13 Comparisons of snow water equivalent in 1996 at Subnivean Snow Laboratory at Niwot Ridge watershed, CO.

Figure 14 Comparison of measured and modeled albedo at the USU drainage farm.